scientific reports

Check for updates

OPEN

Methods for increasing productivity of AC-electrospinning using weir-electrode

Ondrej Batka[1]✉, Josef Skrivanek[1], Pavel Holec[2], Jaroslav Beran[1], Jan Valtera[1] & Martin Bilek[1]

The presented work brings new knowledge in the field of spinning electrodes for AC-electrospinning technology, which is used for producing nanofibrous structures using a solution of polyvinyl butyral. It presents new types of spinning weir-electrodes and describes research on the influence of electrode design parameters on the stability of the spinning process and the productivity of nanofiber production. The multistage spinning electrode is presented in the ratio of stages one to five. Research is also focused on the effect of the parameters of the electric signal used as a source for the spinning electrode on spinning stability and productivity. Observed parameters were voltage level, frequency and shape such as sine wave, rectangle wave and modified sine wave. An analysis of the influence of the spinning conditions on the resulting nanofibrous structure was also performed by analyzing results gained by SEM; the defects were investigated mainly. The results of the research presented in the thesis open up new possibilities for follow-up research in the field of AC-electrospinning.

Keywords Nanofibers, Electrospinning, AC electrospinning, Spinning electrode, Electric field

Electrospinning, whose origin goes back far into history[1–3] and whose gradual development took place from the end of the 19th century to the beginning of the 21st century[4–13], is currently one of the most productive methods used in practice for industrial production of nanofibers. Nanofibrous products offer great potential for application in many fields of human activity[14–24]. This field has been developing dynamically, and the knowledge gained is already being used in practice to a certain extent. Several nanofiber products, or devices for their production, are already available on the market. An example is the Nanospider technology by the Elmarco company, which is used to produce nanofibers intended for various applications worldwide. The Elmarco company developed a new type of needle-less spinning electrode, which uses wire as the electrode where the solution is dispensed using a moving cart, and it is mainly used for industry. However, there are other types of spinning electrodes still commonly used in many applications, and there are many types of research on improving productivity of needle-less electrodes[25–27], or multi-needle electrodes[28]. One of the most common industrial applications where nanofibers are used is the production of filter material with a high efficiency of capturing particles with dimensions of tens or hundreds of nanometers. Another area where nanofibers are expected is tissue engineering, where biodegradable materials are usually used to produce nanofibers[21,29,30]. This area is known, for example, for nanofibrous patches that prevent the anastomic leakage or wound healing[31–33] and are already subjected to in vivo tests[34,35]. In these cases, it is usually a nanomaterial with a flat structure. It is usually a material made of a non-woven base fabric, on which nanofibers are applied, forming a sandwich-type material. Another nanofibrous product in which high potential is assumed is nanofibrous yarn, for example, the dual-functional composite yarns with a nanofibrous envelope developed at the Technical University of Liberec (TUL)[36,37]. In addition, there are functionalized nanofibrous yarns that contain additives that are incorporated among nanofibrous and thus expand their field of use[38]. This material is mainly used in producing filter materials, such as filter fabrics or candle filters[39]. However, it is also expected to be used in medicine in the form of surgical threads with drugs incorporated into the nanofibers[40]. This technology is based on the principle of the Collectorless Alternative Current Electrospinning (AC-electrospinning, or ACES)[41–47], which uses an alternating electric current to form nanofibers. An alternating voltage is applied to the spinning electrode, and an electric field is formed among the electrode itself and air ions. With ACES technology, the presence of an electric-charged collector, which, in this case, arises spontaneously and repeatedly near the spinning electrode,

[1]Department of Textile Machine Design, Faculty of Mechanical Engineering, Technical University of Liberec, Czech Republic, adress: Studentska 1402/2, Liberec 461 17, Czech Republic. [2]Department of Nonwovens and Nanofibrous Materials, Faculty of Textile Engineering, Technical University of Liberec, Czech Republic, adress: Studentska 1402/2, Liberec 461 17, Czech Republic. ✉email: ondrej.batka@tul.cz

is not necessary. This is how we talk about the so-called virtual collector, which is made of electrically charged nanofiber segments. The signs of the electric charges carried bundles of nanofibers formed by the spinning electrode alternate rapidly. Bundles of nanofibers are either positively or negatively charged, with their electric charge corresponding to the corresponding half-wave of alternating current. The action of electric field destabilises a surface of polymer solution, which leads to the formation of polymer nozzles and their subsequent elongation into nanofibers. The creation and disappearance of polymer jets correspond to a change in the polarity of the electric field. Charged nanofibrous bundles immediately behind each other attract each other and create a nanofibrous plume formation. The resulting fibres are clustered, for example, into a linear formation in the form of a strip, which is carried in space by the electric field in the direction of its gradient. Nanofibers created in this way can be collected on many surfaces or objects. It is possible to apply them to a flat base textile, as in the case of DC-electrospinning (DCES), but with advantage they can be directly transformed into a linear structure, such as a yarn or a yarn-like structure[46,47]. In comparison with DCES, the ACES is more productive. By ACES, it is possible to spin many types of polymers in solution, e.g. Polyvinyl butyral[48–50], Polyvinialcohol[29], Polyamide[36,51–54] Polycaprolacton[55,56], Polyacrylonitrile[57], Lignin[58], Polyvinylpyrrolidone[59,60].

Motivation

Developing and optimising devices that can produce nanomaterials with the required topology and structure, both for the laboratory test phase and for industrial use, is necessary for all the mentioned applications. The basis of the technology is always a spinning electrode and an electric input of high electrical voltage. This research aims to determine the influence of electrical quantities such as voltage, frequency and waveform of the electrical signal on the productivity of nanofiber production and the quality of the resulting structure. Furthermore, it is also an effort to influence the productivity of the nanofibres production in the form of a spinning electrode. Finding the dependence of productivity on the mentioned parameters will lead to the efficiency of the production process in terms of the number of nanofibers produced per unit of time; it also has an effect on the installation space of the spinning equipment.

Compared to other technologies for the production of fibre structures, such as high-production meltblown[61–64], electrospinning has the advantage that it is possible to incorporate various materials directly into the fibre structure[50,65–68] thus nanofibrous to functionalised products, for example, for wound healing[69,70]. The diameters of the fibres are also more prominent in Meltblown than in electrospinning, and these are microfibers[63]. Melt-electrospinning technology is also known[71–73], where fibres are produced from a polymer melt, which is an advantage because it does not require solvents, thus increasing ecological sustainability. Experiments show that it is feasible with specific difficulties, but this technology has very low productivity compared to the production of fibres from polymer solutions by electrospinning. It mainly produces microfibers, and a lot of energy is also required to reach and maintain temperatures higher than 200 °C. The advantage of electrospinning of polymeric solutions is the production feasibility of functionalised core-shell fibre by using coaxial electrodes[74–80] possibly produced by ACES. Mixed nanofibrous materials from two or more solution materials are also feasible by special electrodes developed for ACES[81]. This paper's novelty is the research and development of highly effective weirelectrodes for collector-less AC electrospinning technology. The presented electrodes can efficiently produce nanofibrous structures, mainly linear nanofibrous structures like the composite nanofibrous yarn[36] and products such as braided threads[40] or candle filters[39] with high efficiency. The paper also reveals the dependences of productivity and nanofibrous structure quality on many technological parameters.

Methodes

An experiment set-up

The polymeric solution of polyvinyl butyral dissolved in ethanol was used for the experiments ($10\%_{wt}$ PVB Movital B60H in $98\%_{vol}$ ethanol Technisolv). The Trek 50/12 high-voltage amplifier (4) in Fig. 1 was used to supply the voltage signal to the electrode. 1, to the input, the selected signal created by the function generator Owon AG 1022 (6) was fed. Using this device, it is possible to bring any signal with a maximum amplitude of 50 kV, or in the range of ±50 kV to the electrode. The amplifier also allows you to measure the level of output voltage and total current through the outputs in the "OUTPUT MONITOR" Sects. (9, 10). These signals were displayed by a Lecroy waveAce 234 oscilloscope (7), which also allows for determining different types of values (signal amplitude, rms value, mean value). Furthermore, the signal coming out of the function generator (8) was also measured. All productivity measurements were performed in the same way. The nanofibers produced by the electrode (1) moved in the continuous plume (2) towards the rotating drum (3) on which they were deposited, while the time was always measured throughout the spinning period. The manufactured sample (11) was removed and weighed on a VWR® LA Classic balance (12). In most cases, the weight was evaluated in two steps; immediately after finishing spinning and then after drying at the temperature of 50 °C for 30 min. The productivity before drying and after drying in grams per minute was determined from these values. A screw pump was used to supply the polymer solution[82].

FEM model

Autodesk Simulation Mechanical 2017 FEM software was used for simulations of electric fields. The FEM model is in Fig. 2. The task was simulated as a rotationally symmetric model, where the axis of symmetry was the axis of the electrode. For the body of the electrode (4), the metal material with relative permittivity $\varepsilon = 10^9$, was set; for the lid of the beaker (7), polyethene $\varepsilon = 2{,}16$, was specified; glass $\varepsilon = 7{,}6$ for the beaker (6) for the polymer solution on the surface of the electrode (8) and in the beaker (5) $\varepsilon =$ and for the surrounding air by $\varepsilon = 1$. In all cases, a voltage boundary condition (9) with a value of 30 kV and an electrical stiffness of 10^{10} AV^{-1} was imposed on the body of the electrode. A value of 0 V and a stiffness of 10^{10} AV^{-1} were entered at the outer air boundary (3).

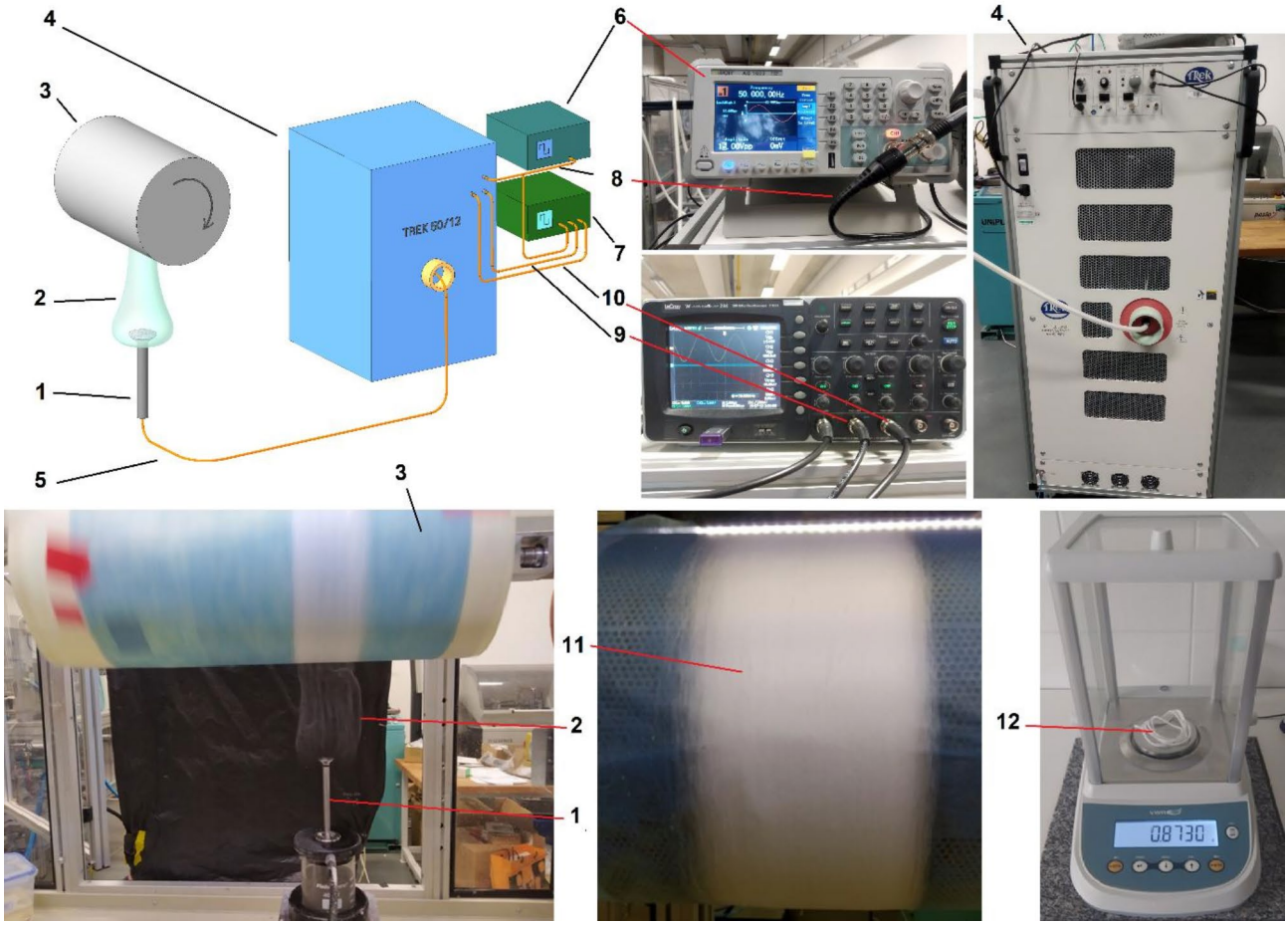

Fig. 1. The principle of experiments; spinning electrode (1), plume of nanofibers (2), colecting drum (3), amplifier Trek 50/12 (4),HV supply to electrode (5), function generator Owon AG 1022 (6), osciloscope Lecroy waveAce 234 (7) generator output signal (8), Voltage measuring signal (9), current measuring signal (10), sample on the colecting drum (11), weighted sample (12).

Weir-electrode

For continuous production of linear nanofibrous products, such as nanofibrous yarn by ACES was by, our team at TUL[83] developed Weir-electrode, shown in Fig. 3 (a). Figure 3b) shows the principle of the overflow electrode used for AC electrospinning. The body of the electrode (1) consists of a cylindrical part ending in a head, usually conical in shape. Through the polymer solution inlet (2), the polymer solution flows upwards onto the transport surface (3). Furthermore, gravity spreads over the entire surface and overflows over the spinning surface (4), on which a dominant amount of fibres is formed, while not all the flowing solution is spun. This surface is continuously followed by the collecting surface (5), after which the non-fibrous solution continues to flow into the container and is subsequently pumped out. On the spinning surface, after applying a high voltage to the body of the electrode, nanofibers are produced due to the high value of the electric field intensity on this surface, as shown in Fig. 3c). We, therefore, refer to such an electrode as a weir-electrode because its entire surface is flooded with solution. Soaking the whole surface is essential for the stability of AC electrospinning. When the electrode was not flooded, and all the supplied solution was spun, the spinning surface would be clogged with nanofibers attracted by the electrode and the process would gradually end, which can be observed in Fig. 4a), respectively in detail A.

In Fig. 4b) stable spinning from an ideally flooded electrode can be observed. Detail B shows the formation of a Taylor cone[8] precisely in the area of high electric field values. The electrode head can take on different shapes, which affect the spinning process and the productivity of nanofiber production, which is the subject of one of the following chapters.

Increasing productivity of weir-electrode

Effect of voltage, frequency and signal waveform on productivity

When examining the weir-electrode, the effect of electrical parameters such as voltage, frequency, and waveform of the electrical signal applied to the single-stage spinning electrode on nanofiber production's productivity and the nanofibers' structure was observed. Two types of electrical voltage waveforms, sine waveform and

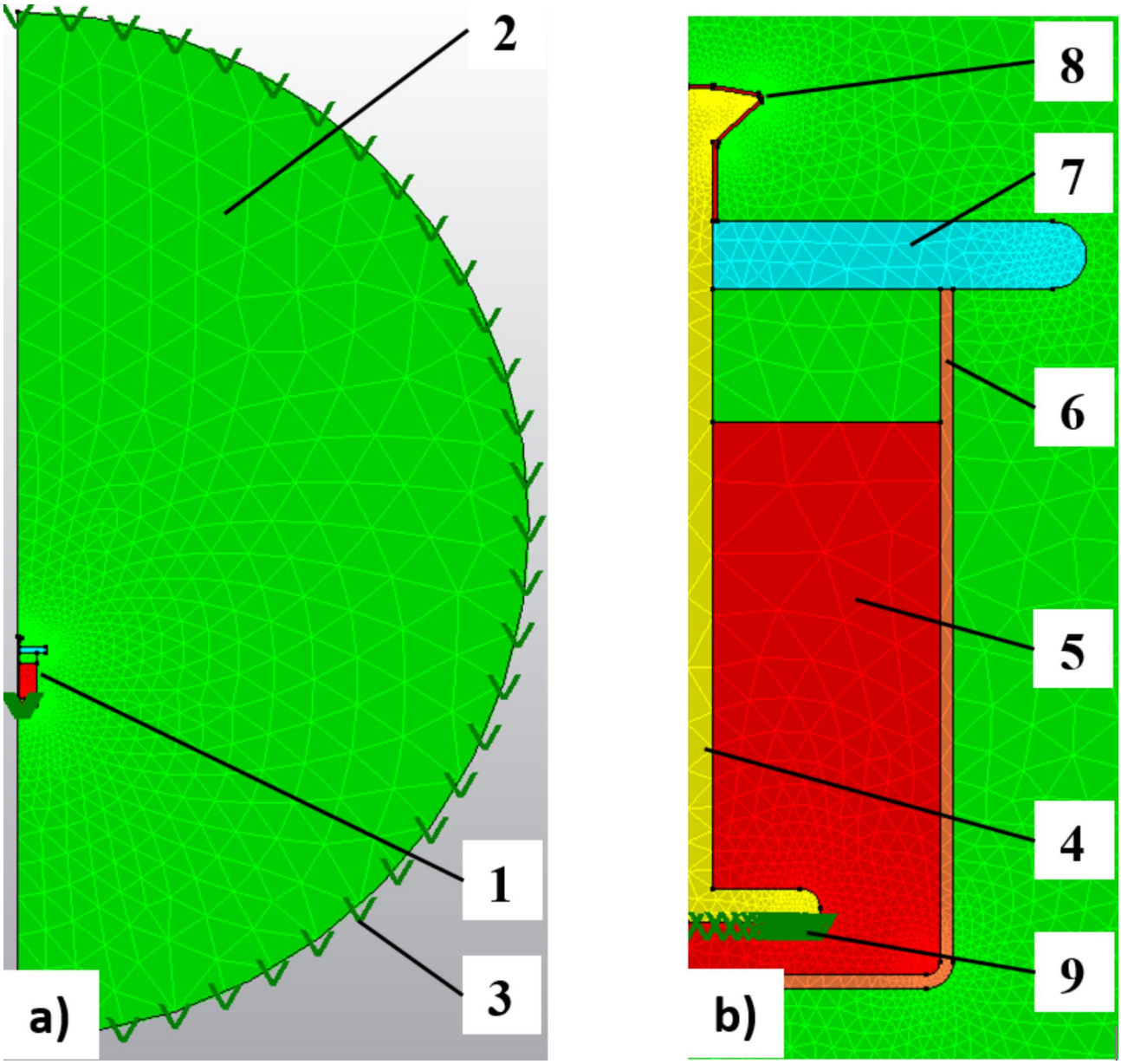

Fig. 2. FEM model (**a**) whole FEM model, electrode assembly 1), air 2), boundary condition 3); (**b**) detail of electrode assembly, electrode 4), polymeric solution in beaker 5), beaker 6), beaker lid 7), polymeric solution on the electrode surface 8), boundary condition on electrode 9).

rectangular waveform with a duty cycle of 50%, were used. In the first part, for both mentioned courses, the attention was focused on investigating the effect of voltage magnitude on productivity in the range of voltage amplitudes of 30 to 50 kV for sine and 35 to 50 kV for rectangular waveform. Figure 5a) shows the dependence of voltage productivity for both waveforms. The graph shows that the productivity increases linearly with the voltage, and the dependence for the rectangular waveform increases with a slightly bigger slope. The square waveform is, therefore, more beneficial for productivity, mainly because it acquires an almost constant value in each half period, while with the sine waveform, the voltage reaches the critical value required for spinning only after a few milliseconds. However, the disadvantage of using a rectangular waveform is that, due to the rapid change in polarity, current peaks occur, which reduces the safety of the device, as they can induce charge into parts of the device or the operator himself, which must be taken into account in the design of the machine. Figure 5b) shows a record of electrical signals recorded by an oscilloscope during the experiments. It can be seen from the figure that current peaks occur in the rectangular waveform (CH3, green). From this point of view, the rectangular waveform is problematic.

In an attempt to limit current peaks but still use the potential of the rectangular waveform, i.e., to extend the time of the supercritical voltage compared to the sinus waveform, a modified signal shape was proposed. Figure 5c) shows an example of the modified sine waveform whose part was limited to the constant value for

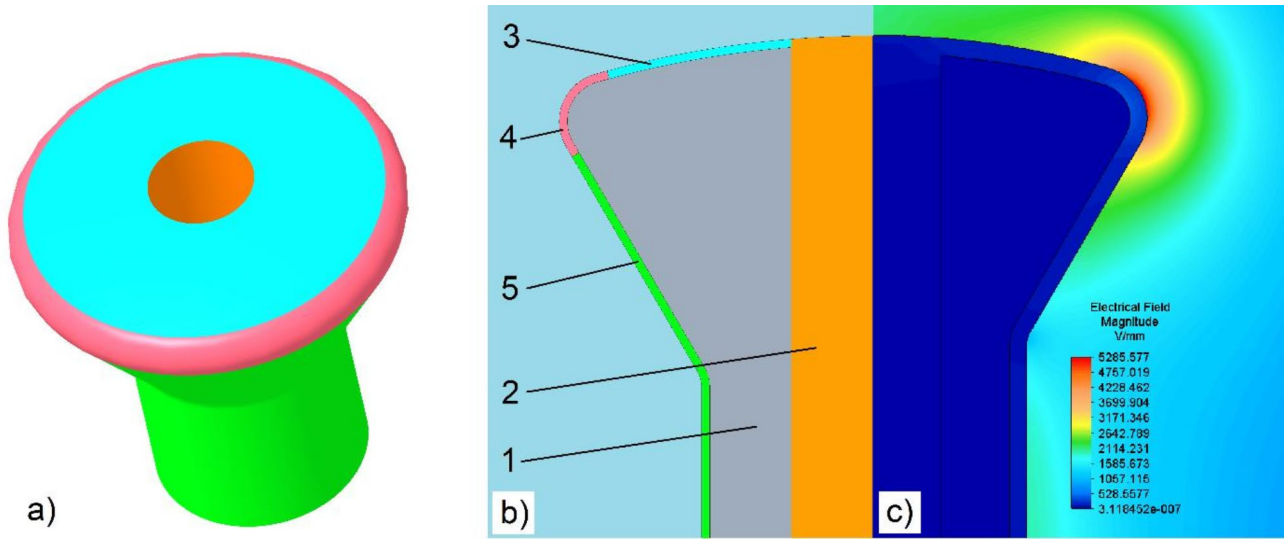

Fig. 3. (**a**) weir-electrode, (**b**) half-section of weir electrode, electrode body (1), inlet (2), transport surface (3), spinning surface (4), colecting surface (5); (**c**) electric field distribution on the electrodes surfaces.

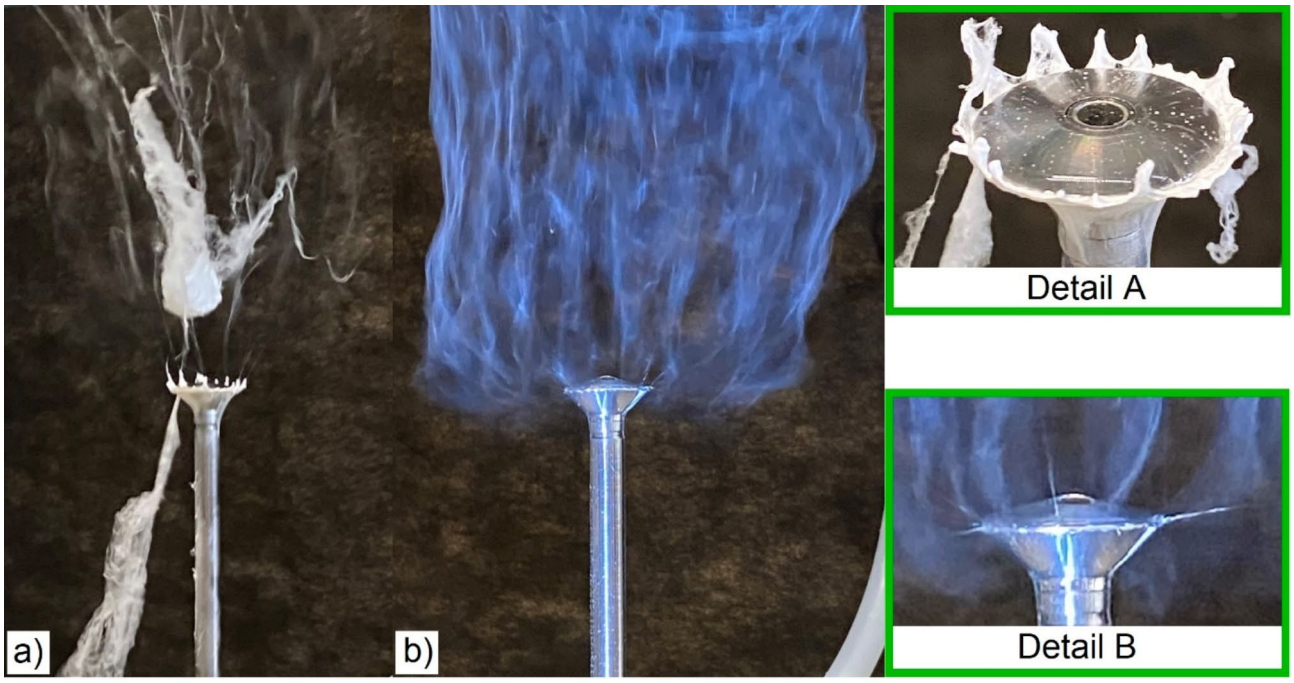

Fig. 4. The AC-electrospinning proces; (**a**) unstable spinning, (**b**) stable spinning.

a certain period. Experiments were performed for three different voltages, namely 40 kV, 45 kV, and 50 kV amplitude values. For each value, the duration of the constant part T_k was gradually changed from 0 s to $T_{0,5}$ s, and for each such course, the productivity was measured. To display the dependence, the ratio of the time of the constant part and the half-period is further marked as Ratio $T_C/T_{0,5}$ was introduced. Figure 5d) shows an example of the waveform record for Ratio $T_C/T_{0,5}$ with value 0,5.

The graph in Fig. 6a) shows the dependence of the measured RMS electrode voltage on ratio $T_C/T_{0,5}$ for all three signal amplitudes, and the graph in Fig. 6b) shows the dependence of productivity on Ratio $T_C/T_{0,}$ for all three AC amplitudes used. The graphs show that as the ratio increases, productivity increases. The graph in Fig. 6c) shows the dependence of the effective value of the electric current measured by the oscilloscope on ratio $T_C/T_{0,5}$ and Fig. 6c) shows the dependence of the maximum current value (peak to peak) on ratio $T_C/T_{0,5}$. It can be seen that the peak values with ratio $T_C/T_{0,5}$ grow non-linearly up to the maximum value, the current to which the amplifier was limited (10 mA) when ratio $T_C/T_{0,5}$ corresponds to the value 1, hence a rectangular waveform.

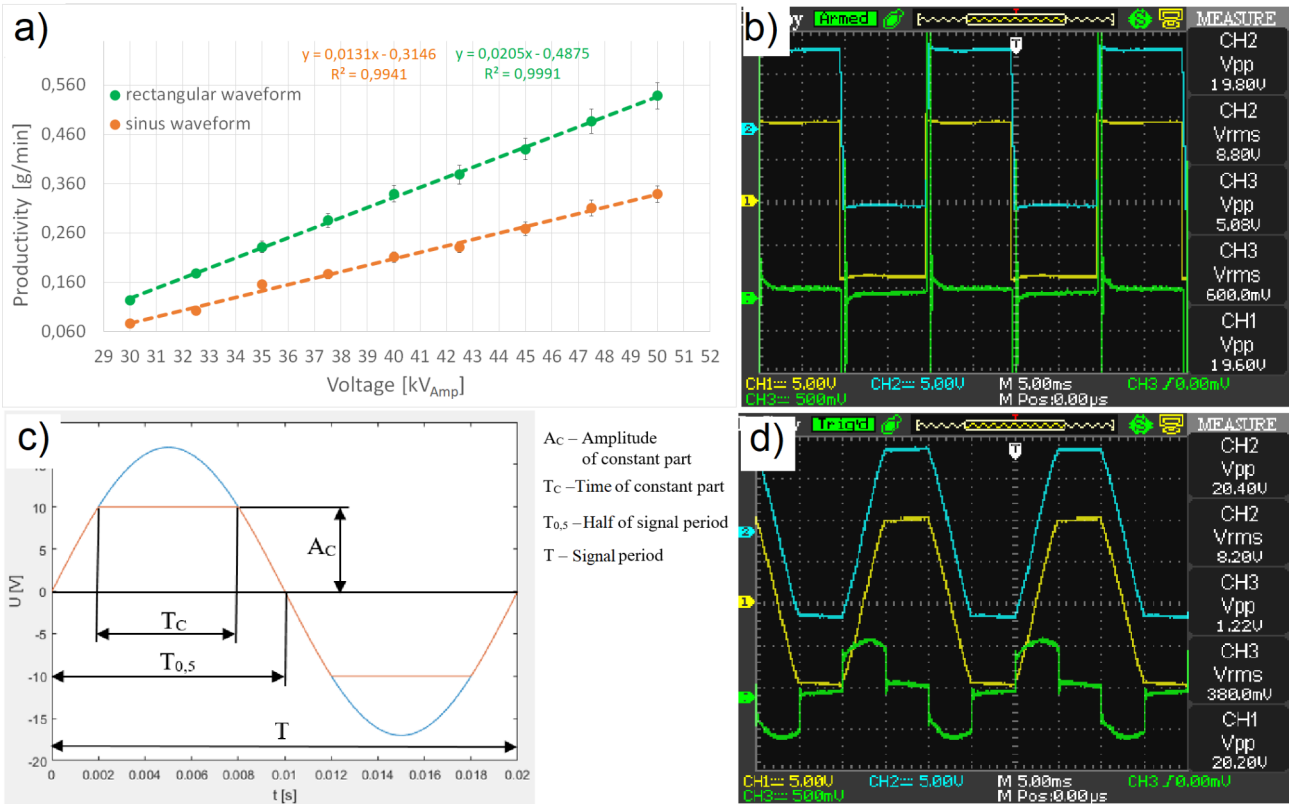

Fig. 5. (**a**) Productivity dependence on voltage, (**b**) measured values for rectangle waveform CH1 – input voltage on TREK CH2 equivalent value of output voltage 5000 V/V CH3 voltage value equivalent to current 0,5 V/mA, (**c**) modified waveform, (**d**) measured values for modified waveform for $T_C/T_{0,5} = 0,6$.

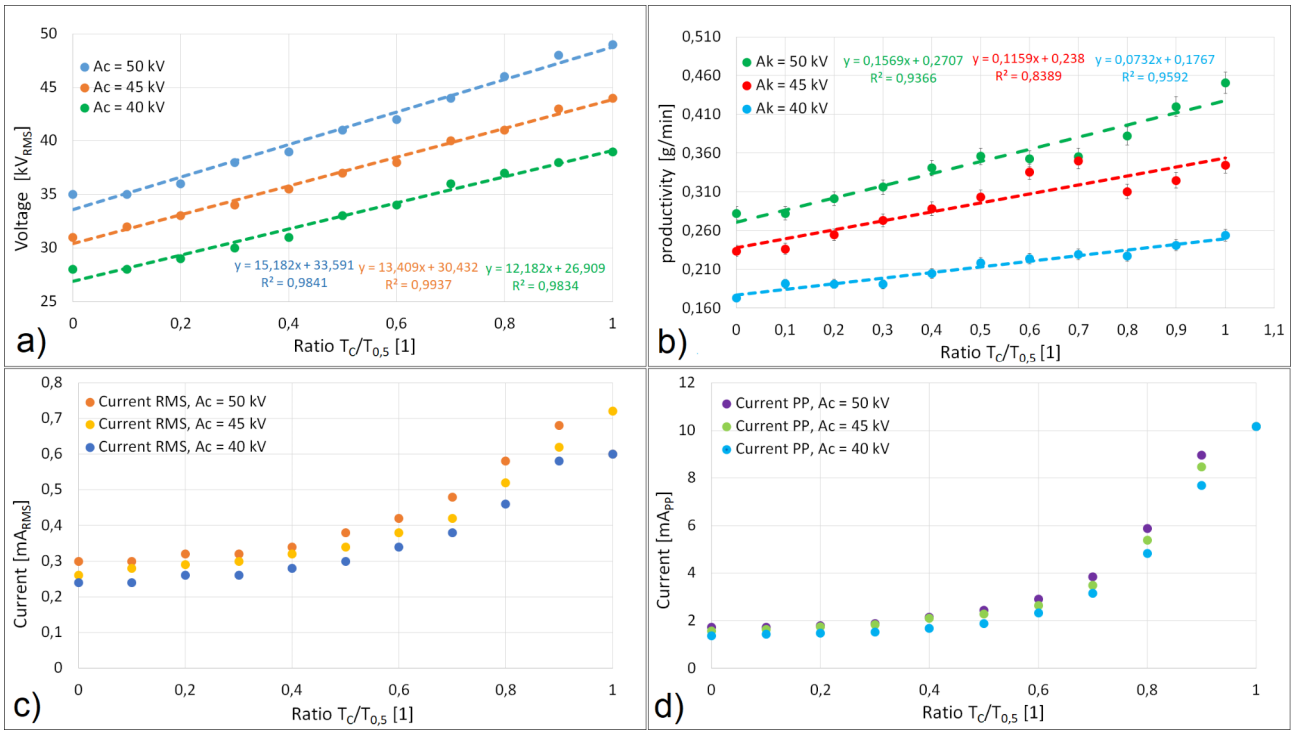

Fig. 6. (**a**) RMS voltage dependence on Ratio, (**b**) RMS productivity dependence on Ratio, (**c**) peak to peak current dependence on Ratio, (**d**) RMS current dependence on Ratio.

Effective values also grow non-linearly, which is shown in Fig. 6d). However, it is clear from the comparison that, especially for values close to 1, the difference between the effective and the peak value is significant, and current peaks are also formed in these cases. The results show that the signal modified this way is usable up to the Ratio = 0,7.

Furthermore, attention was focused on the effect of the frequency of electrical voltage on productivity. Each frequency dependence for a sinusoidal waveform was measured for three different voltages with amplitudes of 40 kV, 45 kV and 50 kV and for a rectangular waveform at 40 kV and 45 kV. The relative humidity in the spinning chamber was 40%, and the temperature was 25 °C. The graph in Fig. 7a) shows the dependence of productivity on frequencies for different voltages of a sinusoidal waveform. It can be seen from the graph that productivity increases with increasing frequency, but the difference between productivity values before and after drying also increases. At a frequency of 125 Hz and a voltage of 40 kV, the productivity's magnitude after the fibres' drying was less than half of the original value. At higher voltages, the difference is even more significant. For example, at a frequency of 95 Hz, at a voltage of 40 kV, the difference between the values is 0.22 g/min, which corresponds to 41.5 per cent of the original value; at a voltage of 45 kV, the difference is 0.33 g/min (45.8%) and at voltage 50 kV 0.49 g/min (49.5%). It follows that at higher frequencies, the produced nanofibrous structure contains a certain amount of solvent, which, as it turned out from the pictures taken by SEM, can negatively affect the final structure. The images are shown in Fig. 8. At frequencies higher than 95 Hz for voltages of 45 kV and 50 kV, the productivity measurement was no longer evaluated because there were clear drops or even entire strips of solution directly in produced samples. It can also be observed in the SEM images that the structure for these parameters shows significant defects. The evaluation of the quality of the resulting structure is presented below. The graph in Fig. 7b) shows the dependence of productivity on frequency for a rectangular waveform. In the graph, behaviour similar to that of the sinusoidal waveform can be observed; as the frequency increases, productivity increases, and so does the difference between the value before and after drying. At frequencies and voltages higher than those shown in the graph, drops of non-fibrous solution formed and degraded the sample. The table in Fig. 7c) shows the nanofiber quality of voltage and frequency combinations for sinus waveform. The quality was divided into four groups: excellent, acceptable, non-acceptable and unusable. However, this is a subjective evaluation based on long-term practice; in particular, the number of defects and the proportion of microfibers, which are considered undesirable in the structure of nanofiber products, are monitored. In conclusion, suitable combinations of voltage and frequency were experimentally found, at which point the quality of the produced nanofibrous structure was of sufficient quality. Regarding productivity, the most suitable combination is a frequency of 70 Hz at a voltage of 50 kV when a productivity of (0,45 ± 0,02) g/min was achieved. It was found that with increasing frequency, the proportion of residual solvent contained in the produced samples increases, considerably degrading the nanofibrous structure at a specific combination of frequencies and voltages. A possible explanation for this phenomenon can be found in the study of the theory of the formation of the Taylor cone. In the first stage of Taylor cone formation, the surface of the polymer solution is deformed to the maximum sharpness of the cone. When a certain amount of solvent is released, a conductive channel is briefly formed, and the charge is partially discharged. This process is repeated until the density and

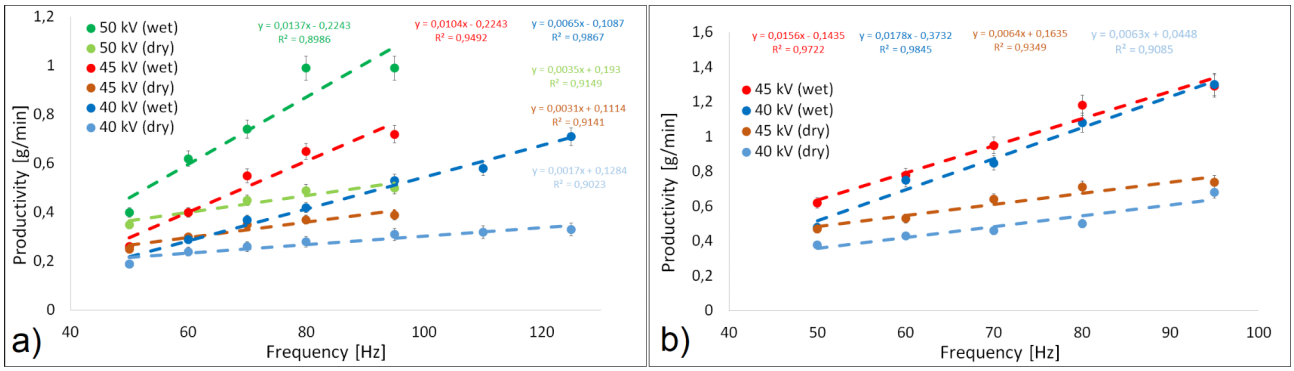

c)

Voltage [kV_{Amp}]	Frequency [Hz]								
	50	60	65	70	75	80	90	100	110
40	excellent	excellent	excellent	excellent	acceptable	acceptable	non-acceptable	non-acceptable	unusable
45	excellent	excellent	acceptable	acceptable	acceptable	non-acceptable	non-acceptable	unusable	unusable
50	excellent	excellent	acceptable	acceptable	non-acceptable	non-acceptable	non-acceptable	unusable	unusable

Fig. 7. (**a**) productivity dependence on frequency for sine waveform, (**b**) productivity dependence on frequency for rectangle waveform, (**c**) table of fibers qualities, **excellent** – standard nanofibrous structure without defects, **acceptable** – nanofibrous structure with an insignificant amount of defects - small drops or an insignificant presence of microfibers. The structure is still very usable, **non-acceptable** – nanofibrous structure with more defects - Considerably large drops, greater presence of microfibers. The use is debatable, **unusable** – a large number of defects - a significant proportion of microfibers, a large number of drops, in some samples the fibers are glued into a single foil. Use is probably excluded for the intended applications.

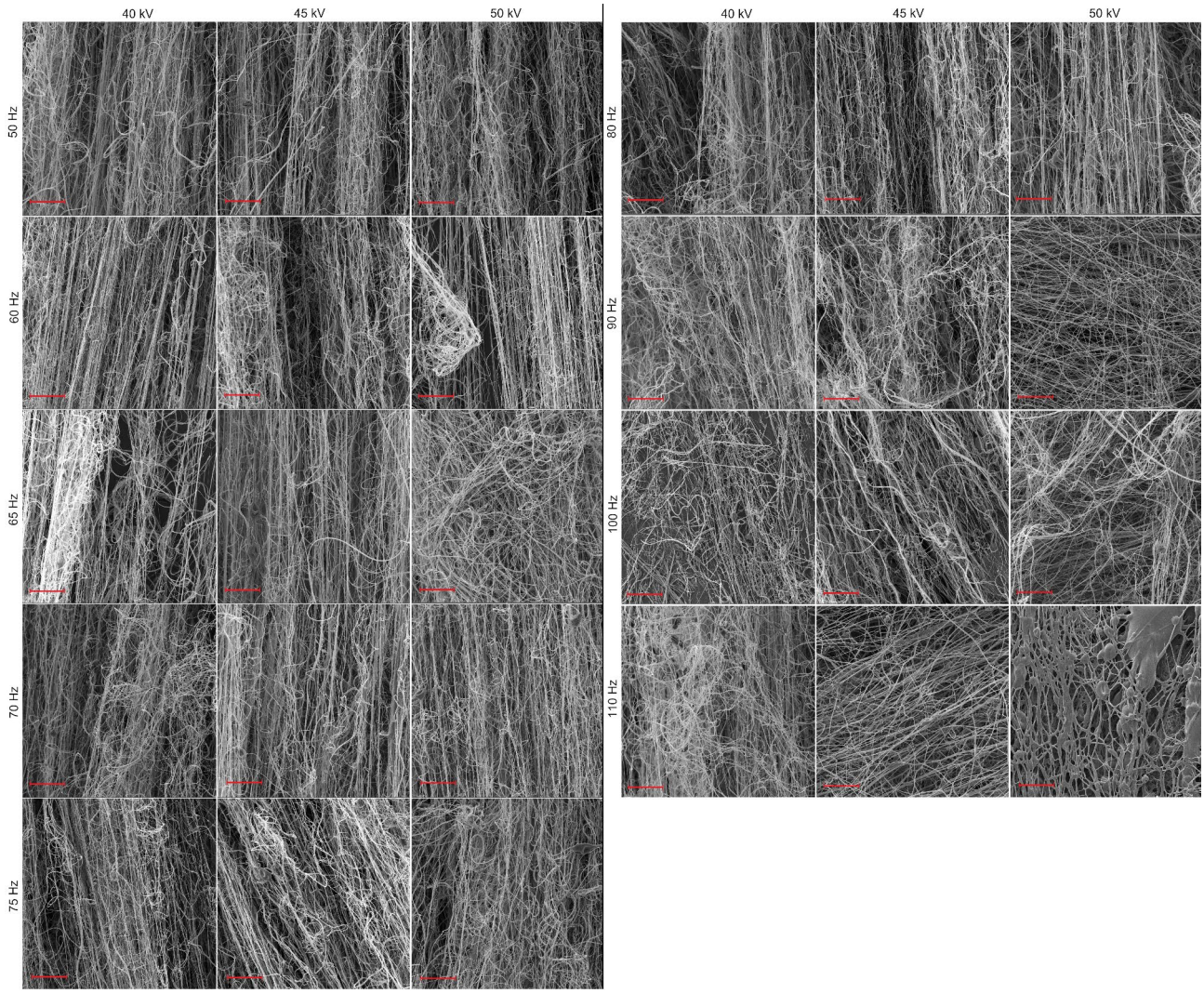

Fig. 8. SEM pictures of structure depending on voltage and frequency, scale bar is 50 µm.

viscosity of the solution are optimal for the formation of a liquid jet and the formation of a Taylor cone[8,84]. This process requires a specific time, which, in the case of AC-electrospinning, must be less than the half-period of the signal. Therefore, the solution must be optimally prepared to reach this criterion. Therefore, apparently, for higher frequencies, the solution is not optimal, and to a large extent, in some places of the polymer surface, the solvent is sprayed, and no fibres are formed. The frequency effect was already observed in previous research in other experiments for other polymeric solutions[85–87]. However, the problem of residual solvent and its effect on the fibre structure was not described.

Effect of electrode geometry on productivity

The electrode with the design parameters shown in Fig. 9a) was subjected to the electric field simulation and subsequently to the experimental productivity measurement, while the diameter of the electrode, further diameter D and the radius of rounding, further radius R, were changed. Figure 9b) shows a set of electrodes with different diameters D and radius R. Experiments were performed for a sinusoidal waveform of the signal on the electrode with an amplitude of 40 kV at a relative humidity in the spinning chamber of 31% and a temperature of 24 °C. Figure 9c) and 9 d) show the graphs of the electric field intensity dependence on radius R, respectively diameter D. It follows from the dependence that the electric field intensity on the spinning surface decreases with the size of the diameter D, and the radius R. Figure 9e) and 9 f) show individually measured dependencies of productivity. It follows from the dependences that with an increasing radius R at a constant diameter D, the productivity decreases slightly (Fig. 9e)) and with an increasing diameter D at a constant radius R, the productivity increases (Fig. 9f)). Looking at the results of the simulations, a decreasing trend can also be observed in the case of the dependence of the electric field intensity on the radius R.

In both cases, the dependence trends on the radius size decreases. However, in the case of dependence on the diameter D, productivity, depending on the size of the diameter D, increases in contrast to electric field intensity. The explanation could be the influence of two factors. The first is that as the diameter D increases, the

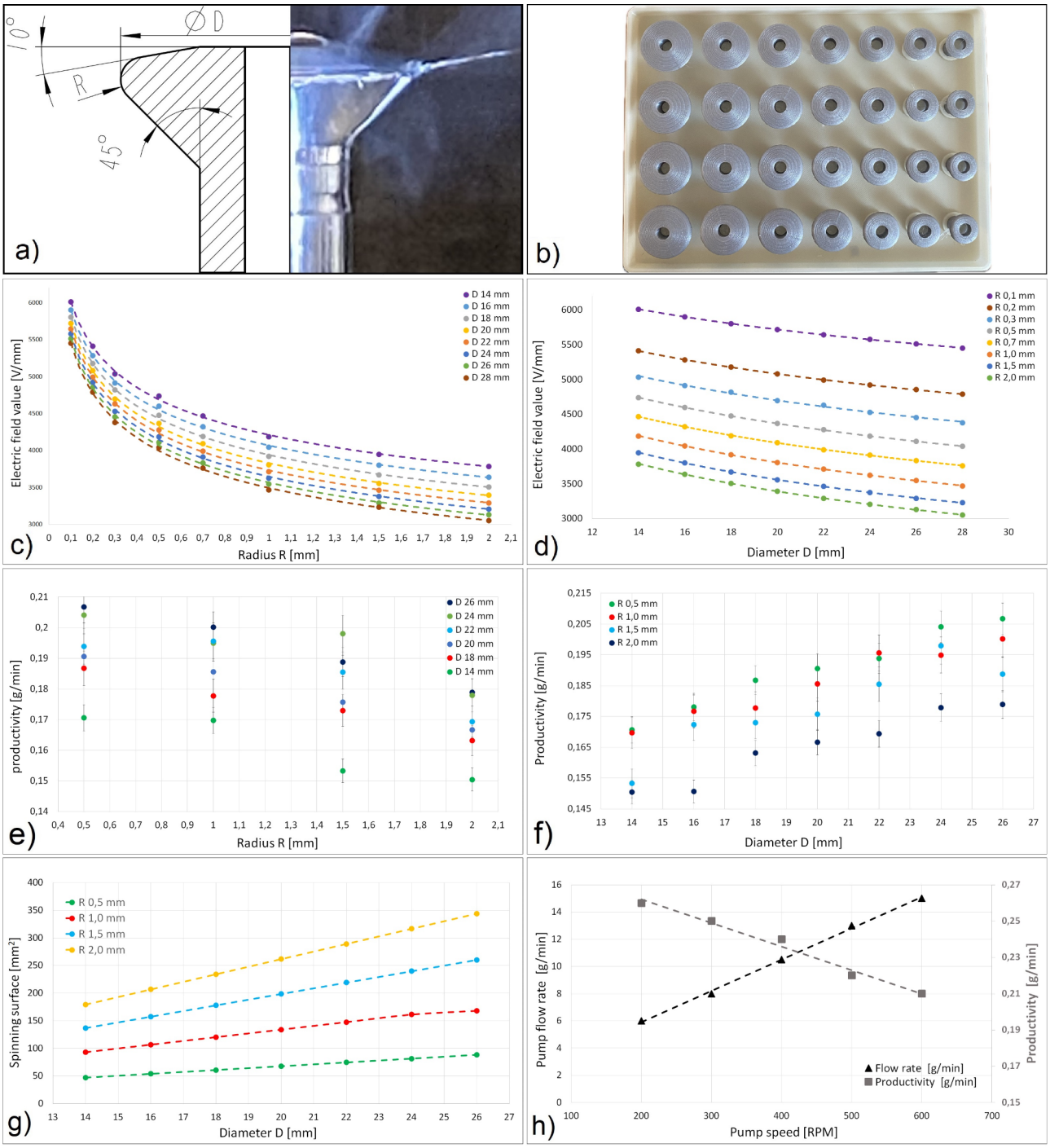

Fig. 9. (**a**) dimensional parameters of the electrode, (**b**) set of testing electrodes, (**c**) electric field dependence on radius R, (**d**) productivity dependence on radius R, (**e**) electric field dependence on diameter D, (**f**) productivity dependence on diameter D,.

size of the spinning surface of the electrode increases, as shown in the graph in Fig. 9g), and thus, the number of Taylor cones on the spinning surface increases and more nanofibers are produced. The second is that the same dosing was used in all measurements. In this case, when the area increases by changing the diameter of the electrode covered by the polymer solution, the thickness of the polymer layer will decrease. It was found that productivity decreases with the thickness of the polymer layer on the electrode. Figure 9h) shows the dependence of productivity on the speed of the screw pump, respectively, on the flow rate, from which it follows that the productivity decreases with the flow rate. It can be assumed that the thickness of the polymer layer on the spinning surface increases with the flow rate. Thus, both factors affect productivity more than electric field strength.

Effect of multistages electrodes

Experiments were also focused on the effect of the number of stages and the spacing of individual steps on productivity. The multistage electrodes used in the experiments were gradually created by assembling different diameters and numbers of stages of the basic conical shape of the electrode. A total of five electrodes with varying numbers of stages were assembled, which were immediately connected to each other. In such an arrangement, the structurally given distance of adjacent stages was 15 mm. An electrode with two, three, four, and five stages was assembled, and experiments for a single-stage electrode were also performed simultaneously for comparison. For each electrode, experiments were carried out for five different electrode voltages for a sine signal at a frequency of 50 Hz. The relative humidity in the spinning chamber was 25%, and the temperature was 23 °C. Figure 10a) – e) shows the snapshots of the experiments. It is possible to observe in the images that, in all cases, the spinning proceeds relatively stably. For the lowest applied voltage of 40 kV, the spinning was less stable at the last stage from the top in the case of the five-stage electrode (Fig. 10e). Similar problems with spinning stability at the lower stage were observed for the highest voltage used, namely 50 kV. In the case of a voltage value of 40 kV, the electric field intensity on the lower stage is not high enough. In the case of a voltage of 50 kV, with a high probability, there is a lack of polymer solution in the last stage.

Figure 10f) shows the dependence of productivity on the number of electrode stages for all applied voltages. The graph shows that productivity increases as the number of degrees increases. In all cases, the dependence shows a quadratic course, which indicates that the maximum possible productivity occurs at a certain number of degrees. This is most evident at a voltage of 40 kV for a five-stage electrode. This is because the electric field intensity is not high enough at the last stage; difficulties with spinning stability at this stage were observed anyway. It is also shown that the proportion of residual solvent increases with increasing number of stages. Figure 10g) shows the dependence of productivity on voltage for all five electrodes for samples in the dried state. Also, in this case, productivity increases linearly with voltage.

Furthermore, experiments were carried out with a two-stage and three-stage electrode, in which the spacing between the individual stages were changed. In the case of a three-stage electrode with a spacing other than the basic one, i.e. 15 mm, the process was unstable; the fibres were difficult to form from the lower stage or had difficulty moving upwards to become part of the nanofiber plume. Therefore, the productivity was not evaluated, and the experiments focused only on the two-stage electrode. Two combinations of the diameters of the individual stages were used. In one case, the diameter of both stages was the same (22 mm); in the other, the first stage had a diameter of 14 mm and the second 26 mm. During the initial trials, it was found that the

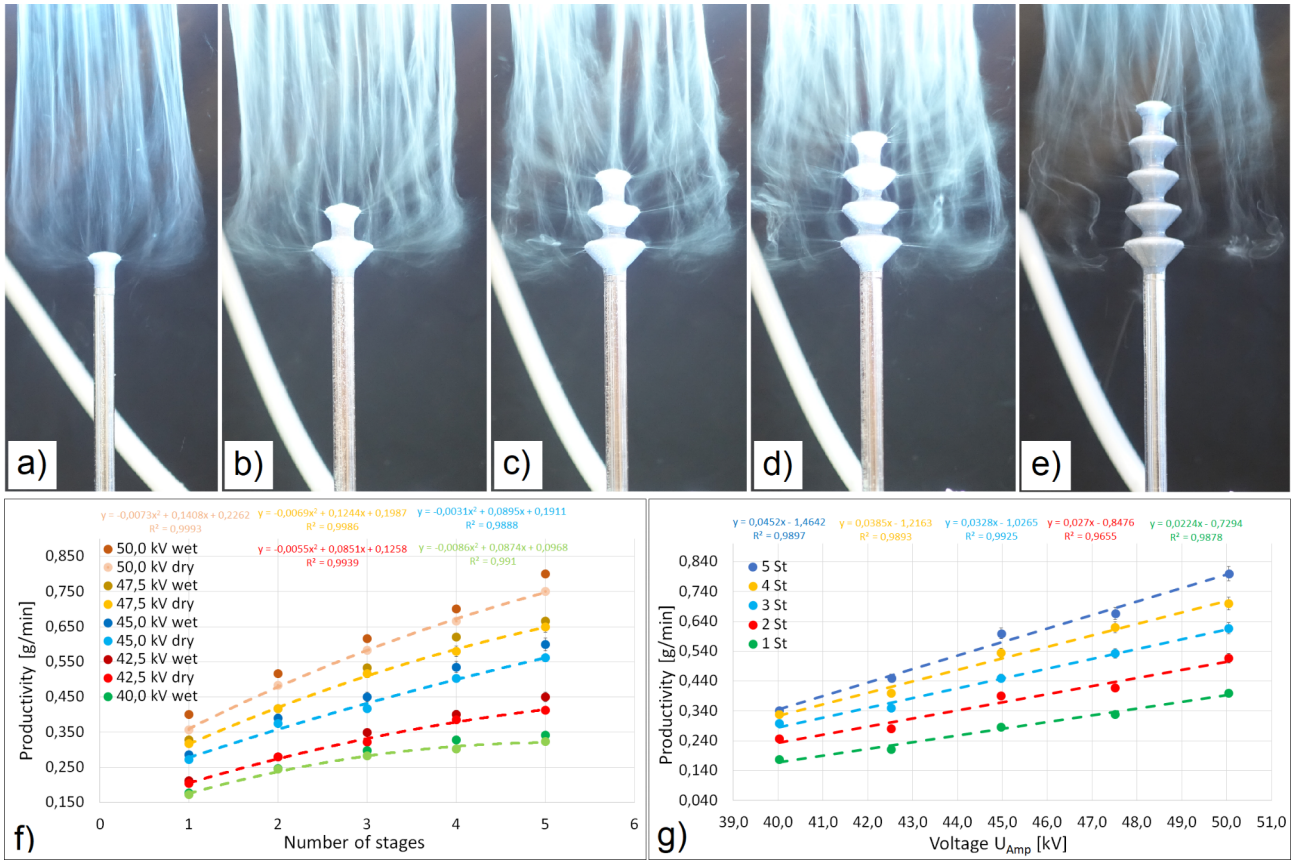

Fig. 10. (**a**) single-stage electrode, (**b**) two-stage electrode, (**c**) three-stage electrode, (**d**) four-stage electrode, (**e**) five-stage electrode, (**f**) productivity dependence on number of steps, (**g**) productivity dependence on voltage.

variant with the same diameters was unsuitable because, at spacing larger than 25, the fibres produced in the second stage had considerable difficulty rising upwards. This phenomenon can be observed in Fig. 11e), f). Figure 11d) shows the process on an electrode with a spacing of 25 mm. Figure 11a), b), and c) offer a variant of the electrode with different diameters for three different stage spacing. It can be seen that, in this case, the fibres that are produced at the lower stage move upwards and become part of the plume. However, for electrodes with a spacing larger than 65 mm, a loss of stability of fibre formation from the lower stage was still observed. Furthermore, the productivity was measured for several spacing values and voltage values on the electrode for a two-stage electrode with different diameters. The relative humidity in the spinning chamber was 35%, and the temperature was 25 °C.

Figure 11g) shows the dependences of productivity on spacing for four different voltages. The graph shows that productivity shows an increasing dependence on the stage spacing, but there is a specific limitation, and in some cases, increasing the spacing is undesirable. At 40 kV and 50 kV, spinning could be stably operated with electrodes with a spacing of up to 45 mm. In the case of a voltage of 40 kV for spacing larger than 45 mm, spinning on the lower stage no longer occurred, and productivity was dropped. One of the possible explanations can be that for such a low voltage, the electric field intensity at the lower stage is not high enough for the formation of fibres. Spinning did occur in the case of a voltage of 50 kV, but the fibres produced on the lower stage had problems progressing upwards. At 42.5 kV and 45 kV voltages, similar problems appeared only at spacings higher than 65 mm. Spinning did occur, but frequent breakdowns in process stability were observed in the lower stage. A more significant number of solution droplets also appeared in the produced structure; therefore, the productivity was no longer evaluated. In this case, an insufficient amount of polymer solution affects the spinning conditions in the lower stage.

Conlusion

The presented weir spinning electrode showed the ability to produce nanofibers from polymer solutions with high productivity. Experiments have revealed that productivity increases with increasing electrical voltage and frequency of the electrical signal. However, the quality of the manufactured structure is also affected by voltage and frequency; it is proven that with increasing voltage and frequency, the quality deteriorates and thus reduces usability. This is due to the content of the solvent in the produced structure, which causes the dissolution of the produced nanofibers. It should be noted that this phenomenon can be influenced by the concentration of the solution and also by its type. The effect of frequency and voltage will differ for other materials and solvents, requiring further extensive research. When using a rectangle waveform, there is greater productivity than with a sine waveform at the same amplitude values. However, the disadvantage of the rectangular signal is a more significant current load on the source due to rapid polarity changes and a higher risk of corona discharges, which reduces the safety of operation, especially when using flammable solvents. The multistage electrodes can be used to increase productivity, i.e., the number of spinning surfaces. However, it follows from the experiment that it is necessary to ensure a sufficient voltage so that there is sufficient intensity of the electric field at all spinning stages. Furthermore, it ensures a sufficient supply of polymer solution at individual stages. With many stages, the last stages are not sufficiently supplied by polymeric solution. From this point of view, it will be necessary to optimise the multistage electrode further so that all stages have the same conditions for spinning, especially the same coverage with the polymer solution and the same electric field intensity. This requires extensive research on multistage electrodes. With multistage electrodes, the spacing between individual stages also plays a role. Increasing the spacing makes it possible to increase productivity, but even here, limits were found that are related to the supply and, thus, to the ability of the electric wind to transport the fibres in the desired direction. It is necessary to point out that the presented results relate to a narrow profile of the issue, especially what concerns the type of polymer solution and, thus, its concentration. It is likely that for different solutions of different

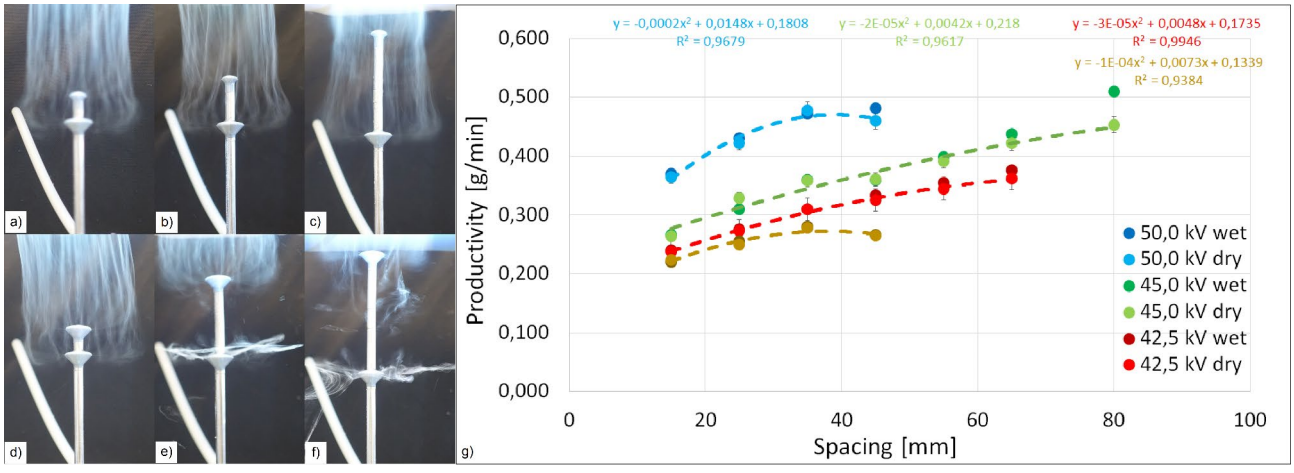

Fig. 11. (**a**) 1st stg. 14 mm 2nd stg. 26 mm pitch 15 mm, a) 1st stg. 14 mm 2nd stg. 26 mm pitch 65 mm, a) 1st tg. 14 mm 2nd stg. 26 mm pitch 80 mm, (**d**) identical diameters pitch 15 mm, (**e**) identical diameters pitch 65 mm, (**f**) identical diameters pitch 80 mm, (**g**) productivity dependence on the pitch.

concentrations with different solvent systems, the behavior of the spinning process will be different, and it will be necessary to adapt the technology adjustment in relation to the monitored parameters listed in this paper. In the future, it is also necessary to focus on the ecological aspects of electrospinning technology. The general effort in spinning technology emphasising sustainability and ecology is the highest possible concentration of spun material and the lowest possible solvent concentration in the spinning solution[88]. The idealised state would be 100% concentration of the spun material without solvent; in this way, a waste-free product with almost zero emissions would be achieved. To illustrate, when spinning PVB material and the average solution concentration is $10\%_{wt}$, $90\%_{wt}$ of the liquid solution is converted into gaseous ethanol vapours since the inorganic solvent ethanol is used for spinning[89]. Ethanol vapours are extremely flammable and explosive and must be handled environmentally and safely. In more giant factories, having an air vent for vapours in the catalytic combustion equipment behind the spinning box is standard practice. The vapours are burned, creating an additional environmental burden for the air, as emissions are created during combustion, and it is also necessary to burn life-giving oxygen as a condition for combustion. In general, it can be stated that the associated technological operations increase the ecological and economic burden of electrospinning[90].

Data availability

The data are available upon request. Contact Ondrej Batka (ondrej.batka@tul.cz).

Received: 15 July 2024; Accepted: 9 October 2024
Published online: 14 October 2024

5 References

1. William, G. I. L. B. E. R. T. De Magnete, Magneticisque Corporibus, et de magno magnete Tellure; Physiologia nova, Plurimis & Argumentis, & Experimentis Demonstrata. London: Peter Short, 1600. in.
2. Gray, S. II. A letter concerning the electricity of water, from Mr. Stephen Gray to Cromwell Mortimer, M. D. Secr. R. S. *Philos. Trans. R. Soc. Lond.* **37**, 227–260 (1997).
3. X. Part of a letter from Abbè Nollet, of the Royal Academy of Science at Paris, and F. R. S. to Martin Folkes Esq; President of the same, concerning electricity. *Phil. Trans. R. Soc.* 45, 187–194 (1748).
4. Boys, C. V. On the Production, Properties, and some suggested Uses of the Finest Threads. *Proc. Phys. Soc. London* 9, 8 (1887).
5. Cooley, J. F. Apparatus for electrically dispersing fluids. (1902).
6. Morton, W. J. Method of dispersing fluids. (1902).
7. Anton, F. Process and apparatus for preparing artificial threads. (1934).
8. I. Taylor, G. Disintegration of water drops in an electric field. *Proc. Royal Soc. Lond. Ser. Math. Phys. Sci.* **280**, 383–397 (1964).
9. Taylor, G. I. & Van Dyke, M. D. Electrically driven jets. *Proc. Royal Soc. Lond. Math. Phys. Sci.* **313**, 453–475 (1969).
10. Reneker, D. H. & Chun, I. Nanometre diameter fibres of polymer, produced by electrospinning. *Nanotechnology*. **7**, 216–223 (1996).
11. Cengiz, F. & Jirsak, O. The effect of salt on the roller electrospinning of polyurethane nanofibers. *Fibers Polym.* **10**, 177–184 (2009).
12. Jirsak, O. et al. A method of nanofibres production from a polymer solution using electrostatic spinning and a device for carrying out the method. (2009).
13. Petras, D. et al. Method for spinning the liquid matrix, device for production of nanofibres through electrostatic spinning of liquid matrix and spinning electrode for such device. (2009).
14. Ibrahim, H. M. & Klingner, A. A review on electrospun polymeric nanofibers: production parameters and potential applications. *Polym. Test.* **90**, 106647 (2020).
15. Lannutti, J., Reneker, D., Ma, T., Tomasko, D. & Farson, D. Electrospinning for tissue engineering scaffolds. *Mater. Sci. Engineering: C.* **27**, 504–509 (2007).
16. *Electrospun Nanofibers for Energy and Environmental Applications*.
17. Madheswaran, D. et al. Composite yarns with antibacterial nanofibrous sheaths produced by collectorless alternating-current electrospinning for suture applications. *J. Appl. Polym. Sci.* **139**, (2022).
18. Azmil Arif, M. W. et al. Electrospinning of Polyacrylonitrile Nanofibres and Applications in membrane Distillation Technology: a review. *Int. J. Nanoelectronics Mater.* **15**, 183–207 (2022).
19. Li, J., Liu, Y. & Abdelhakim, H. E. Drug delivery applications of Coaxial Electrospun nanofibres in Cancer Therapy. *Molecules* **27**, (2022).
20. Bendkowska, W. Use of nanotechnology in the textile industry. *Przeglad Wlokienniczy* 17–21 (2003).
21. Ngiam, M., Hayes, T. R., Dhara, S. & Su, B. Biomimetic apatite/polycaprolactone (PCL) nanofibres for bone tissue engineering scaffolds. *Key Eng. Mater.* **II**, 330–332 (2007).
22. Owida, A., Xiu, M. M., Wong, C. S. & Morsi, Y. S. Electrospinning of nanofibres for construction of vital organ replacements. in 585–587 doi: (2006). https://doi.org/10.1109/ICONN.2006.340685
23. Kalayci, V., Ouyang, M. & Graham, K. Polymeric nanofibres in high efficiency filtration applications. *Filtration*. **6**, 286–293 (2006).
24. Lawson, C., Sivan, M., Pokorny, P., Stanishevsky, A. & Lukáš, D. Poly(ϵ-Caprolactone) nanofibers for Biomedical Scaffolds by High-Rate Alternating Current Electrospinning. in **1** 1289–1294 (2016).
25. Wei, L., Sun, R., Liu, C., Xiong, J. & Qin, X. Mass production of nanofibers from needleless electrospinning by a novel annular spinneret. *Mater. Design.* **179**, 107885 (2019).
26. Wei, L. et al. Experimental investigation of process parameters for the filtration property of nanofiber membrane fabricated by needleless electrospinning apparatus. *J. Ind. Text.* **50**, 1528–1541 (2021).
27. Wei, L. et al. Process investigation of nanofiber diameter based on linear needleless spinneret by response surface methodology. *Polym. Test.Bold"*>*110*, 107577 (2022).
28. Wei, L. et al. Multiple-jet needleless Electrospinning Approach via a Linear Flume Spinneret. *Polymers*. **11**, 2052 (2019).
29. Homer, W. J. A. et al. Assessment of thermally stabilized electrospun poly(vinyl alcohol) materials as cell permeable membranes for a novel blood salvage device. *Biomaterials Adv.* **144**, 213197 (2023).
30. Blanquer, A. et al. A novel bifunctional multilayered nanofibrous membrane combining polycaprolactone and poly (vinyl alcohol) enriched with platelet lysate for skin wound healing. *Nanoscale*. https://doi.org/10.1039/d3nr04705a (2024).
31. Kingham, P. T. & Pachter, L. H. Colonic Anastomotic Leak: risk factors, diagnosis, and treatment. *J. Am. Coll. Surg.* **208**, 269 (2009).
32. Qu, H., Liu, Y. & Bi, D. Clinical risk factors for anastomotic leakage after laparoscopic anterior resection for rectal cancer: a systematic review and meta-analysis. *Surg. Endosc*. **29**, 3608–3617 (2015).
33. Meyer, J. et al. Reducing anastomotic leak in colorectal surgery: the old dogmas and the new challenges. *World J. Gastroenterol.* **25**, 5017–5025 (2019).

34. Klicova, M. et al. Novel double-layered planar scaffold combining electrospun PCL fibers and PVA hydrogels with high shape integrity and water stability. *Mater. Lett.* **263**, (2020).
35. Rosendorf, J. et al. Double-layered nanofibrous patch for prevention of anastomotic leakage and peritoneal adhesions, experimental study. *Vivo*. **35**, 731–741 (2021).
36. Valtera, J. et al. Fabrication of dual-functional composite yarns with a nanofibrous envelope using high throughput AC needleless and collectorless electrospinning. *Sci. Rep.* **9**, (2019).
37. Beran, J. et al. A linear fibre formation with a case of polymeric nanofibres enveloping the supporting linear formation constituting the core, the method and equipment for its production. (2017).
38. Skrivanek, J. et al. Production of modified Composite Nanofiber yarns with functional particles. *ACS Omega*. **8**, 1114–1120 (2023).
39. Homoláč, J., Jašková, D. & Valtera *J. Candle Filter.* (2021).
40. Madheswaran, D. et al. Braided threads with AC electrospun nanofibers for hygienic and medical applications - production and properties. in 252–257 doi: (2021). https://doi.org/10.37904/nanocon.2021.4355
41. Kessick, R., Fenn, J. & Tepper, G. The use of AC potentials in electrospraying and electrospinning processes. *Polymer*. **45**, 2981–2984 (2004).
42. Sarkar, S., Deevi, S. & Tepper, G. Biased AC electrospinning of aligned polymer nanofibers. *Macromol. Rapid Commun.* **28**, 1034–1039 (2007).
43. Maheshwari, S. & Chang, H. C. Assembly of Multi-stranded Nanofiber threads through AC Electrospinning. *Adv. Mater.Bold"*>*21*, 349–354 (2009).
44. Pokorny, P. et al. Alternating current electrospinning method for preparation of nanofibrous materials. in 302–304 (2013).
45. Pokorny, P. et al. New variant of electrospinning: a collector-less method. in (2013).
46. Lukas, D. et al. Effective AC needleless and collectorless electrospinning for yarn production. *Phys. Chem. Chem. Phys.* **16**, (2014).
47. KOCIS, L. et al. Method for production of polymeric nanofibers by spinning of solution or melt of polymer in electric field, and a linear formation from polymeric nanofibers prepared by this method. (2019).
48. Qin, M. et al. Electrospun polyvinyl butyral/berberine membranes for antibacterial air filtration. *Mater. Letters: X*. **10**, 100074 (2021).
49. Lou, Z. et al. Electrospun PVB/AVE NMs as mask filter layer for win-win effects of filtration and antibacterial activity. *J. Membr. Sci.* **672**, 121473 (2023).
50. Kuželová Košťáková, E. et al. Electrospun Polyvinyl Butyral Nanofibers Loaded with Bismuth Oxide nanoparticles for X-ray shielding. *ACS Appl. Nano Mater.* **6**, 5242–5254 (2023).
51. Kalous, T., Holec, P., Jirkovec, R., Lukas, D. & Chvojka, J. Improved spinnability of PA 6 solutions using AC electrospinning. *Mater. Lett.* **283**, 128761 (2021).
52. Holec, P., Kalous, T., Pokorny, P., Batka, O. & Skrivanek, J. ALTERNATING CURRENT ELECTROSPINNING OF PA 6 USING ADDITIVES IN FORM OF OXOACIDS. in 143–147 doi: (2021). https://doi.org/10.37904/nanocon.2021.4329
53. Kalous, T. et al. The optimization of Alternating Current Electrospun PA 6 solutions using a visual analysis system. *Polymers*. **13**, 2098 (2021).
54. Holec, P. et al. The potential for the Direct and Alternating Current-Driven Electrospinning of Polyamides. *Nanomaterials*. **12**, 665 (2022).
55. Sivan, M. et al. Plasma treatment effects on bulk properties of polycaprolactone nanofibrous mats fabricated by uncommon AC electrospinning: a comparative study. *Surf. Coat. Technol.* **399**, 126203 (2020).
56. Sivan, M. et al. AC electrospinning: impact of high voltage and solvent on the electrospinnability and productivity of polycaprolactone electrospun nanofibrous scaffolds. *Mater. Today Chem*. **26**, 101025 (2022).
57. Paulett, K. et al. Effect of nanocrystalline cellulose addition on needleless alternating current electrospinning and properties of nanofibrous polyacrylonitrile meshes. *J. Appl. Polym. Sci.* **135**, (2018).
58. Mikeš, P. et al. The Mass Production of Lignin Fibres by means of needleless Electrospinning. *J. Polym. Environ.*https://doi.org/10.1007/s10924-020-02029-7 (2021).
59. Balogh, A. et al. Alternating current electrospinning for preparation of fibrous drug delivery systems. *Int. J. Pharm.* **495**, 75–80 (2015).
60. Farkas, B. Corona alternating current electrospinning_ a combined approach for increasing the productivity of electrospinning. *Int. J. Pharm.* (2019).
61. Goswami, B. C. *Developments in spunbonding and meltblown nonwoven structures*. 363 (25 pages). (1990).
62. Dutton, K. C. Overview and analysis of the meltblown process and parameters. *J. Text. Appar. Technol. Manage.* **6**, (2009).
63. Drabek, J. & Zatloukal, M. Meltblown technology for production of polymeric microfibers/nanofibers: a review. *Phys. Fluids*. **31**, 091301 (2019).
64. Bhat, G. S., Malkan, S. R. & Islam, S. Chapter 6 - Spunbond and meltblown web formation. in *Handbook of Nonwovens (Second Edition)* (ed. Russell, S. J.) 217–278Woodhead Publishing, doi: (2022). https://doi.org/10.1016/B978-0-12-818912-2.00001-X
65. Das, M. et al. Aligning TiO2 nanofiber for high ionic conductivity in cellulose acetate gel electrolytes. *Mater. Chem. Phys.* **314**, (2024).
66. Zhang, M. et al. Aligned nanofibers incorporated composite solid electrolyte for high-sensitivity oxygen sensing at medium temperatures. *J. Mater. Sci. Technol.* **181**, 189–197 (2024).
67. Talib Al-Sudani, B. et al. A novel antioxidant and antimicrobial food packaging based on Eudragit ®/collagen electrospun nanofiber incorporated with bitter orange peel essential oil. *LWT* 193, (2024).
68. de Barros, H. E. A. et al. Development of poly(vinyl alcohol) nanofibers incorporated with aqueous plant extracts by solution blow spinning and their application as strawberry coatings. *J. Food Eng.* **363**, (2024).
69. Do Pham, D. D. et al. Novel lipophosphonoxin-loaded polycaprolactone electrospun nanofiber dressing reduces Staphylococcus aureus induced wound infection in mice. *Sci. Rep.* **11**, 17688 (2021).
70. Arumugam, M. et al. Multifunctional silk fibroin and cellulose acetate composite nanofibers incorporated with palladium and platinum nanoparticles for enhanced wound healing: comprehensive characterization and in vivo assessment. *Colloids Surf., a* **684**, (2024).
71. Lyons, J. & Ko, F. Feature article: Melt Electrospinning of polymers: a review. *Polym. News*. **30**, 170–178 (2005).
72. Kong, C. S., Jo, K. J., Jo, N. K. & Kim, H. S. Effects of the spin line temperature profile and melt index of poly(propylene) on melt-electrospinning. *Polym. Eng. Sci.* **49**, 391–396 (2009).
73. Morikawa, K. et al. Melt Electrospinning Polyethylene fibers in Inert Atmosphere. *Macromol. Mater. Eng.* **305**, 2000106 (2020).
74. Reznik, S. N., Yarin, A. L., Zussman, E. & Bercovici, L. Evolution of a compound droplet attached to a core-shell nozzle under the action of a strong electric field. *Phys. Fluids*. **18**, 062101 (2006).
75. Song, T., Zhang, Y. Z. & Zhou, T. J. Fabrication of magnetic composite nanofibers of poly(ε-caprolactone) with FePt nanoparticles by coaxial electrospinning. *J. Magn. Magn. Mater.* **303**, e286–e289 (2006).
76. Bazilevsky, A. V., Yarin, A. L. & Megaridis, C. M. Co-electrospinning of core–Shell fibers using a single-nozzle technique. *Langmuir*. **23**, 2311–2314 (2007).
77. Moghe, A. K. & Gupta, P. B. S. Co-axial Electrospinning for Nanofiber structures: Preparation and Applications. *Polym. Rev.* **48**, 353–377 (2008).
78. Liao, I., Chew, S. & Leong, K. Aligned core–shell nanofibers delivering bioactive proteins. *Nanomedicine*. **1**, 465–471 (2006).

79. Vysloužilová, L. et al. Needleless coaxial electrospinning: a novel approach to mass production of coaxial nanofibers. *Int. J. Pharm.* **516**, 293–300 (2017).
80. Skrivanek, J. et al. Design of electrode for coaxial electrospinning. in 303–307 (2016).
81. Souček, J., Valtera, J. & Kalous, T. Electrode for continuous production of composite nanofiber material using ac-electrospinning method. *2017-October* 378–383 (2018).
82. Beran, J., Lukáš, D., Pokorný, P., Kalous, T. & Valtera, J. A method of producing polymer nanofibres by electric or electrostatic spinning of a polymer solution or melt, a spinning electrode for this method, and a device for the production of polymer nanofibres fitted with at least one such spinning electrode. (2019).
83. Beran, J. et al. Method for producing polymeric nanofibers by electrospinning a polymer solution or melt, a spinning electrode for performing the method and a device for producing polymeric nanofibers equipped with at least one such spinning electrode. (2020).
84. Lukáš, D. et al. Physical principles of electrospinning (Electrospinning as a nano-scale technology of the twenty-first century). *Text. Prog.* **41**, 59–140 (2009).
85. Farkas, B., Balogh, A., Farkas, A., Marosi, G. & Nagy, Z. K. Frequency and waveform dependence of alternating current electrospinning and their uses for drug dissolution enhancement. *Int. J. Pharm.* **586**, 119593 (2020).
86. Sivan, M., Madheswaran, D., Valtera, J., Kostakova, E. K. & Lukas, D. Alternating current electrospinning: the impacts of various high-voltage signal shapes and frequencies on the spinnability and productivity of polycaprolactone nanofibers. *Mater. Design.* **213**, 110308 (2022).
87. Kalous, T. et al. The effect of frequency change on the alternating current electrospinning of polyamide 6 and its productivity. *J. Environ. Chem. Eng.* **11**, 109543 (2023).
88. Malara, A. Environmental concerns on the use of the electrospinning technique for the production of polymeric micro/nanofibers. *Sci. Rep.* **14**, 8293 (2024).
89. Yener, F. & Yalcinkaya, B. Electrospinning of polyvinyl butyral in different solvents. *e-Polymers* 13, (2013).
90. Green Electrospinning. Making Electrospinning Environmentally Friendly. *AZoNano* (2023). https://www.azonano.com/article.aspx?ArticleID=6540

Acknowledgements

The paper has been elaborated with financial support of TUL in the framework of Institutional Support for Longterm Development of Research Organizations.

Author contributions

OB did experiments, prepared data and figures and wrote the main manuscript; JS did experiments and reviewed the manuscript; PH made the SEM images of nanofibrous structures, and JB, JV and MB supervised the research.

Declarations

Competing interests

The authors declare no competing interests.

Additional information

Correspondence and requests for materials should be addressed to O.B.

Reprints and permissions information is available at www.nature.com/reprints.

Publisher's note Springer Nature remains neutral with regard to jurisdictional claims in published maps and institutional affiliations.